IJNRD.ORG ISSN : 2456-4184
INTERNATIONAL JOURNAL OF NOVEL RESEARCH AND DEVELOPMENT (IJNRD) | IJNRD.ORG
An International Open Access, Peer-reviewed, Refereed Journal

Phyto mediated Biogenic synthesis of Silver Nanoparticles from stem bark extracts of *Phyllanthus reticulates* an approach to assessment of Antibacterial, antioxidant, and cytotoxic prospective

D. Meera[1]*, P. Koteshwar[2], and CH. Venkataramana Devi[1]*
[1]* Department of Biochemistry, UCS, Osmania University, Hyderabad.
2. Technical Assistant, ICAR, Rajendranagar, Hyderabad.

ABSTRACT

Phyllanthus reticulatus belongs to the family Phyllanthaceae, profusely existing in India. It's a globally used medicinal plant in treating diverse ailments, predominantly for gastrointestinal disorders and diabetes. Yet the trend of Phyto-mediated silver nanoparticle synthesis is occurring from sources that are eco-friendly and non-hazardous and are of great importance in preventing environmental and health problems. Therefore, the current study aimed to evaluate the efficiency of *Phyllanthus reticulatus* stem bark as a reducing and stabilizing agent for silver nanoparticle synthesis, characterization, and evaluation of antibacterial activity, antioxidant, and cytotoxic activity. The synthesized nanoparticles were characterized by performing UV-Vis spectrophotometer, SEM, and TEM. UV visible spectroscopic analysis revealed the Surface Plasmon Resonance (SPR) ultimately the reduction of AgNO3 to silver nanoparticles is confirmed. The FTIR indicated -OH, -C=C-, and alkane as the functional groups responsible for the stabilization of the silver nanoparticle formed. The morphological assessment of silver nanoparticles formed confirmed by SEM and TEM analysis particles are spherical in shape with an average particle size of 28.80nm. The EDX analysis ascertained that the silver surface plasmon resonance at 2.8–3.2 keV was confirmed. The XRD study revealed the crystalline nature of the synthesized nanoparticles. Subsequently the antibacterial activity of silver nanoparticles prepared from stem bark extracts of *Phyllanthus reticulatus*. Our study substantiated that bark extracts of *Phyllanthus reticulatus* act as an excellent capping agent for forming silver nanoparticles and showed immense biological activities. Consequently, we studied *Phyllanthus reticulatus* bark extracts AgNPs can be used as an antimicrobial, antioxidant, and cytotoxic investigation in treating many medical complications. We anticipate our work will pave a significant way in the area of nanotechnology and nanomedicine.

Keywords: Silver nanoparticles, Biosynthesis, Characterization, Antibacterial activity, Antioxidant and cytotoxic activity, and *Phyllanthus reticulatus* stem bark.

Introduction:

The demand for silver nanoparticles is increasing globally due to their wide application in medicine, food, electronics, and agricultural industries. Day by day, Nanotechnology is becoming a novel and promising area in Pharmacognosy and phytomedicine. It is mostly distributed with a developing material size range from 1 to 100nm

(Kumar et al., 2014). The activity of nanoparticles arises from the quantum size effect that is remarkably different from bulk form. Nanoparticles are attributed in diverse areas for instance electronic, chemical, and mechanical industries, catalysts, drug carriers, sensors, magnetic, and pigments viz., Zahoor et al. (2021). Currently, Nanoparticles are considered as a sustainable antimicrobial agent with notable potential for the assessment of antibiotic therapy. The trend for developing plant-based silver nanoparticles as a novel antimicrobial and Phyto therapeutic agent with better efficacy is yet to continue. The foremost reason for the usage of photo-based silver nanoparticles are environmentally friendly as reducing agents. Therefore, the necessity for intense improvement of environmental, high-yield, and safer practices to supersede the chemical reduction approach is very important (Satyavathi et al., 2019). This instigated biosynthesis, which uses plant extract, microorganisms, and yeast as reducing agents. Correspondingly, plants are a promising source of reducing agents in nanoparticle synthesis is becoming the easiest way. *Phyllanthus reticulatus* is a medicinal plant that is more often found around the globe, traditionally used as an antihypertensive, aphrodisiac, insecticidal, anticancer, antidiabetic, and antimicrobial agent. There are reports proving its medicinal use. However, limited data is available on the preparation of silver nanoparticles. Therefore, we aimed to study the characterization, antimicrobial, antioxidant, and anticancer activity study of silver nanoparticles synthesized using *Phyllanthus reticulatus bark* extract as a reducing agent. Ours is the first study for the preparation of the silver nanoparticles of *Phyllanthus reticulatus stem bark* extract silver nanoparticles and the enumeration of its bio efficacy.

MATERIALS AND METHODS:

Materials: Silver nitrate (AgNO3), Muller Hilton Agar, 3- (4,5-dimethylthiazol-2-yl)-2,5-diphenyltetrazolium bromide (MTT), 2,2-diphenyl-1-picrylhydrazyl (DPPH), and dimethyl sulfoxide (DMSO) were procured from HiMedia. All other chemicals used were of analytical grade and high purity and were procured from reputed firms.

Plant material:

The diseased free *Phyllanthus reticulatus* stem bark was collected from the botanical garden of Osmania University, Hyderabad, Telangana. The stem bark of *P. reticulatus* collection and Identification took place in the month of February 2018.

Preparation of Silver nanoparticles from the Stem bark extracts of *P.reticulatus*:

The stem bark of *P. reticulatus* was cleaned properly, shade air-dried, and pulverized into fine particles by using a mechanical grinder. The extraction of stem bark was done by using a magnetic stirrer, an amount of 200 g pulverized powder of stem bark of *P.reticulatus* into a beaker containing double distilled water at room temperature. The mixture was left for 48 hours for proper extraction with proper agitation at 3-hour intervals. The solution was filtered and the filtrate obtained was transferred into an amber-colored sample bottle and kept in the refrigerator at 4^0C for further analysis. Synthesis of silver nanoparticles using *P.reticulatus* stem bark extract 1 mM silver nitrate (AgNO3) solution was prepared. The prepared AgNO3 solution and *P.reticulatus* stem extract were thoroughly mixed together in a ratio of 1:10. The mixture was heated in a beaker at 45^0C and stirred continuously at 800 rpm via a magnetic stirrer. The color of the solution changed to reddish brown after 2 hours. The mixture was filtered and the filtrate obtained was stored in a sample bottle and kept in the refrigerator prior to further analysis.

Results and Discussion:

This study investigated the biosynthesis of *Phyllanthus Reticulatus* Poir. Stem bark extract-based silver nanoparticles (PR-AgNPs) and evaluation of the antibacterial, antioxidant, and cytotoxic potential of nanoparticles using the stem bark extract of *P.reticulatus*.

Phytochemical Analysis.

Various phytochemical constituents in the aqueous stem bark extract of P.reticulatus responsible for the reduction and capping of silver nanoparticles are qualitatively analyzed. From the phytochemical screening of the *P.reticulatus* aqueous stem bark extract, it was found to be a good source of secondary metabolites, as shown in Table 1. These phytochemicals may be responsible for the reduction of silver and acting as a capping agent to prevent aggregation of and provide stability to the nanoparticles. The majority of the phytochemicals extracted in polar solvents are polar in nature and play a significant role in the synthesis of nanoparticles.

Table 1. Qualitative Phytochemical Screening of Aqueous Leaf Extracts of P.reticulatus

phytoconstituents	aqueous stem bark extract
tannins	+
flavonoids	–
alkaloids	+
triterpenoids	+
phenol	+
saponins	+

+Presence; −Absence.

Synthesis of Stem Bark Silver Nanoparticle

In this proposed study Phyllanthus reticulatus stem bark was first time used for the biosynthesis of silver nanoparticles. The preliminary detection of the prepared nanoparticles was based on the color changes of the solutions by visual observation. The solution containing AgNO3 and stem bark changed from light brown to deep brown color after the autoclaving indicating the formation of AgNPs. The formation of the silver nanoparticles was further assessed by a UV-vis spectrophotometer. When subjected to autoclaving, the metal ions are reduced in the presence of the *Phyllanthus reticulatus* stem bark biopolymer from Ag^{+1} to Ag^{0}.

Fig 1: *Phyllanthus reticulatus* stem bark extract in the conical flask containing solutions of silver nitrate

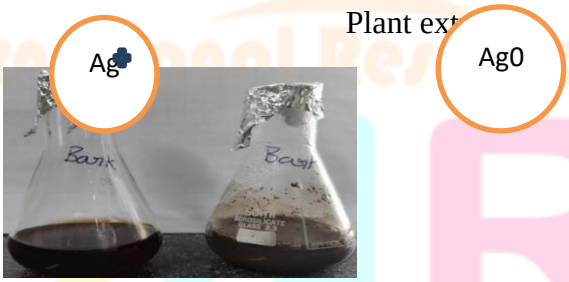

Fig 2: Green Synthesis of Conversion of Silver (Ag) to Silver Nanoparticle (SNPs)

The reduction of silver ions into silver nanoparticles was analyzed by spectral data obtained by using a UV-Vis spectrophotometer analysis which is the common technique for qualitative analysis of nanoparticles. It showed an absorbance peak around 440 nm which confirms the specificity for silver nanoparticles.

Effect of stem bark extract

The concentration of stem bark extract played an important role in the synthesis of nanoparticles. With the increase in the concentration of bark extract from 0.2% – 1.0%, the absorbance values increased until they reached the optimal value of one percent. These results revealed that bark extract concentration is directly proportional to the

formation of the nanoparticle. Hence, the nanoparticle for the study was prepared using 1% *Phyllanthus reticulatus* bark extract.

Optical Studies

UV-Vis spectrophotometric analysis

A UV-visible absorption spectra of AgNPs, from Phyllanthus reticulatus stem bark extract of various concentrations (5, 10, and 15 mL), are shown in Figure. The optical analysis is the simplest way to discover the development of Ag NPs from an aqueous mixture of AgNO3 and stem bark extract synthesized. The aqueous AgNO3 was turned into dark brown when Phyllanthus reticulatus stem bark extract was added into the solution mixture. The change in mixture color indicates the formation of AgNPs. The absorption spectra show a peak around 450 nm, indicating Surface Plasmon Resonance (SPR) between electron clouds from the AgNP surface and incident light photons. The absorption peak occurs at 451 nm when the addition of 5 mL stem bark extract, while for 10 mL stem bark extract, the absorption peak shifts to 450 nm, and a further increase in the leaf extract to 15 mL, shows a significant change in the occurrence of absorption peak (at 448 nm) in the spectra. A similar pattern is also observed by various researchers in different stem bark extracts of different concentrations since the obtained results are well agreed with previous reports (Kathiravan, 2018; Gomathi et al., 2018). The variation in the occurrence of absorption peaks plays a vital role in the size of Ag NPs. In this work, the absorption peak shifts towards a shorter wavelength while increasing the extract concentration, due to the reduction of particle size in accordance with the concentration of possible biological reducing agents in the Phyllanthus reticulatus stem bark extract. Moreover, along with the peak shift, the intensities of the peak increase with the increase in extract concentration which can be attributed to the scale of production of Ag NPs increasing. An aqueous solution containing P. reticulatus transformed from light brown to dark brown in the nanoparticles. Characteristically, UV–visible spectral analysis is used to study the surface plasmon resonance (SPR) for Ag nanoparticles as an indicator of first-level confirmation for the generation of nanostructures. A periodic optical absorbance scan of the nanoparticles synthesized was recorded using a UV-vis spectrophotometer. The characteristic surface plasmon resonance was recorded in UV- vis absorption spectra (200-800nm) for the nanoparticle. The Ag nanoparticles showed a distinctive peak at 410nm depicting its typical SPR.

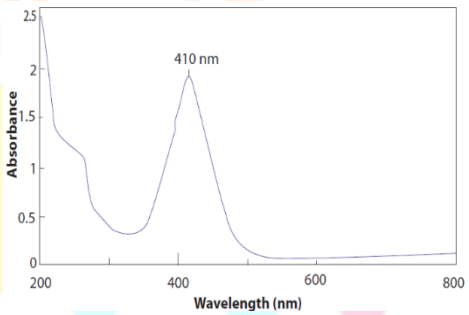

Fig 3: A Schematic representation of absorbance spectra of AgNP prepared from the stem bark of *Phyllanthus reticulatus.*

FTIR Spectroscopic Analysis of Synthesized Silver Nanoparticles

The functional groups responsible for the binding and reduction of silver ions were identified from the FTIR spectra. The FTIR spectra of Phyllanthus reticulatus stem bark extract and synthesized silver nanoparticles revealed similar absorption bands at varying absorption wavelengths (3860.43, 2949.71, 2524.55, 2181.61, 1653.95, 1415.58, and679.54 cm-1 respectively). These peaks in the infrared region correspond to -OH functional groups of phenolic or alcohol, -C-H of alkane, C=C of alkene, and bending vibration of –C-H of alkane respectively. The presence of these functional groups confirmed that Phyllanthus reticulatus stem bark extract contains metabolites that are capable of serving as stabilizing and reducing agents for the synthesized silver nanoparticles. This study

agrees with recent studies that confirm –the OH functional group as a reducing agent in the synthesis of silver nanoparticles.

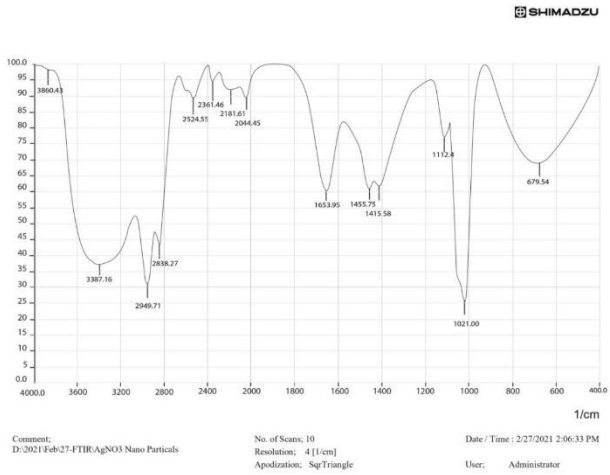

Fig 4: FTIR spectrum of Synthesized silver nanoparticle

Structural Studies

XRD Analysis of Synthesized Silver Nanoparticles

The XRD pattern revealed that the Phyllanthus reticulatus stem bark extract was used as a reducing agent. From the spectra, three distinctive diffraction peaks of 38.07, 44.25, and 76.71 at 20 θ values indexed to the (111), (200), and (311) reflection planes of the face-centered cubic structure of silver. This confirmed that the synthesized silver nanoparticles are crystalline in nature. The occurrence of these peaks also ascertained that the extract contains some organic compounds that are responsible for the reduction of silver ions and stabilization of resultant nanoparticles. The data obtained from the XRD pattern is similar to the finding for green synthesized AgNPs using Ocimum canum by Jayaseelan and Rahuman,2012. Dipankar et al reported the diffraction angle (2 θ 0 at 27.72 o belonged to the face-centered cubic structure of Ag NPs.

The average particle size of AgNPs is calculated using Scherrer's formula from FWHM(full-width half maximum) of predominant peaks.

$$D = 0.94\lambda/\beta \cos\theta$$

Where λ is the wavelength of XRD (1.5406 Å) used in this study, β is the FWHM of the predominant peak, and θ is Bragg's diffraction angle. The average particle size is 31 nm for 5 mL stem bark extract and the value of particle size decreased to 27 nm for 10 mL of leaf extract. The introduction of stem bark extract into the solution mixture further increased to 15 mL, and as a result particle size drastically decreased to 22 nm. This decrease in particle size can be ascribed to the Zener pinning effect; the rapid growth of particles having large defects gives way to stopping the periodic extension of crystallite growth to a large size (Rajkumar et al., 2015).

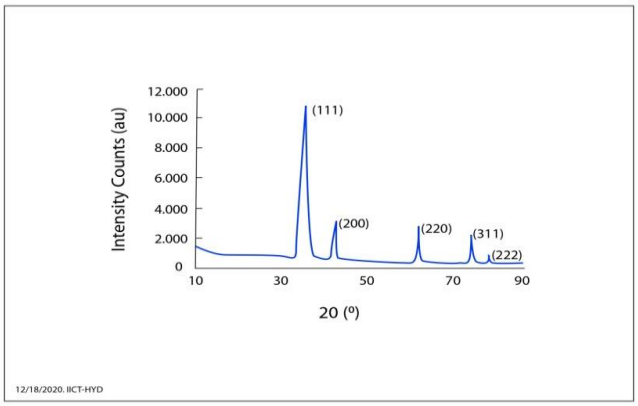

Fig 5: XRD pattern in synthesized silver nanoparticles

Surface Morphological Studies:

SEM Analysis of synthesized silver nanoparticles.

The morphology features of the synthesized silver nanoparticles obtained from SEM analysis are displayed in the SEM micrograph. confirmed a mono-disperse spherical particle. SEM images of 5-, 10-, and 15-mL stem bark extract synthesized AgNPs. The surface morphology of AgNPs is obviously illustrated from the SEM images. In the case of a 5 mL extract of a synthesized sample, most of the particles are undefined shape, because of the combination of the number of particles and only a few of them are roughly spherical shape AgNPs. There are no significant changes observed throughout the SEM image of the 10 mL extract synthesized sample. However, an entirely different morphology is observed by the sample synthesized from 15 mL stem bark extract and the image contains smooth and spherical shape Ag NPs. The majority of the images are having small size Ag NPs. However, we can see large-size particles which can be attributed to the aggregation of a large number of the smallest ones.

EDX Analysis of Synthesized Silver Nanoparticles

The EDX image of the synthesized silver nanoparticles shown in Figure revealed a distinct peak of silver at 3.2–4.2 keV which indicates the reduction of silver ions (Ag+ to Ag0). From the image, it is noticed that the strong energy peaks have emerged and are associated with the anticipated element Ag. Also, there are two other peaks at 0.8 and 1.4 keV corresponding to carbon and oxygen respectively. The atomic percentage of silver, carbon, and oxygen is 47.86% 32.09%, and 20.05% respectively. The signal of carbon might have emanated from the adsorbed components of the coating material of the instrument while the signal of oxygen might have originated from atmospheric oxygen from the air. Previous studies confirmed a typical absorption peak around 2.5 KeV as silver Surface Plasmon Resonance

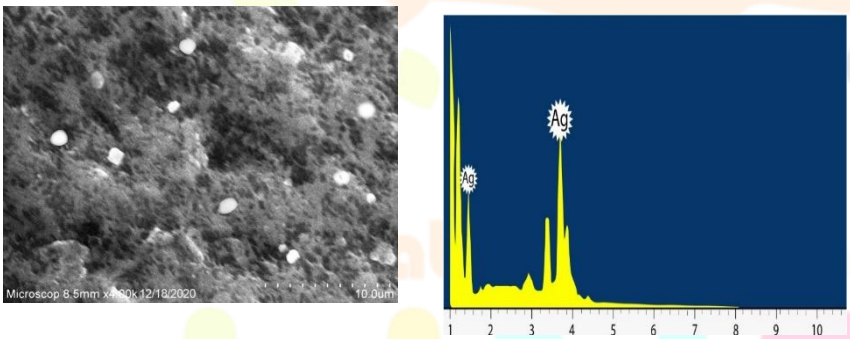

A B

Fig 6: Scanning electron microscopy (SEM) micrographs of silver nanoparticles along with EDX analysis

TEM Analysis of Synthesized Silver Nanoparticles:

The TEM micrograph of the synthesized silver nanoparticles revealed that the synthesized silver nanoparticles are properly dispersed, spherical, and had particle sizes ranging from 18 to 38nm with an average particle size of 28nm Figure shows TEM images of green synthesized AgNPs. TEM analysis clearly illustrates the size and shape of AgNPs. It exposes that Ag NPs are well segregated and mainly spherical in shape. However, a few of them are found to be irregular in shape. From the TEM image, it can be concluded that the AgNPs are nano-size, and roughly spherical in shape.

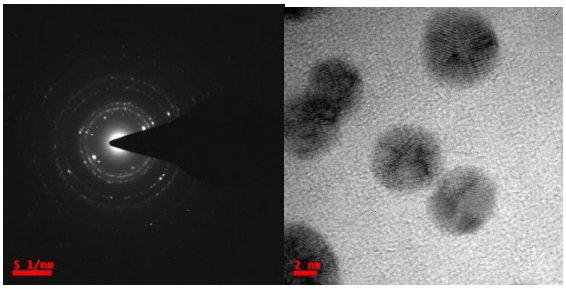

Figure 7: Transmission Electron Microscope (TEM) micrograph of silver nanoparticle

Antibacterial Assay/ Well Diffusion Assay

The well diffusion method was performed to assess the antibacterial activity of the as-synthesized silver nanoparticles. (Ag-NPs). The results depict the zone of inhibition (ZOI). The ZOI measured (mm) with silver nanoparticles against various bacterial strains. After an incubation period for 24 h at 37° C, inhibition of both gram-positive and gram-negative bacterial growth was observed when treated with AgNPs (5 µg mL^{-1}), with ZOI diameter(mm) 14 for *Salmonella typhi, 08* for *S. aureus, 05* for *P. aeruginosa, and 04* for *E.coli* respectively. However, no zones of inhibition were observed for extract even after treatment with concentrations >100 µg mL^{-1} Autoclaved bark which was used as negative control did not show any zone of inhibition in the bacterial strains. The antibiotic amikacin used as positive control displayed 08, 03,03, and 03mm zones of inhibition against *Salmonella typhi, S. aureus, E.coli,* and *P. aeruginosa* respectively. The results exhibited that individual AgNPs exert maximum inhibition in both bacterial strains followed.

Test Organisms	**Stem bark-based silver nanoparticles**	**Agno3**	**Standard (Amikacin)**	**DW (Control-1)**	**Extract (Control-2)**
	Zone of inhibition in mm				
Salmonella typhi	14	03	08	ND	04
Staphylococcus aureus	08	02	03	ND	ND
Pseudomonas aeruginosa	05	02	03	ND	ND
E.Coli	04	02	03	ND	ND

Table 2: Antibacterial activity of the synthesized AgNPs from stem bark aqueous extracts tested against two Gram-positive and two Gram-negative bacterial, ND-Not detected, DW-Distilled water, AgNo3- Silver nitrate and standard-Amikacin

Fig 8: The bacterial culture plates show the zone of inhibition (mm) around wells loaded with various Ag-NPs for Gram-positive bacterial strains (*S. aureus)*, and Gram-negative (*P. aeruginosa, E.coli, and Salmonella typhi*).

Graph

Calculation of %RSA and IC50 From DPPH Assay					
Absorbance measurement data					
S.No	Concentration	Control	Sample	%RSA	IC50
1	10	0.52	0.312	40	6.956569
2	20	0.52	0.291	44.04	16.95657
3	40	0.52	0.228	56.15	36.95657
4	60	0.52	0.18	65.38	56.95657
5	80	0.52	0.14	73.08	76.95657
6	100	0.52	0.075	85.58	96.95657
7	120	0.52	0.035	93.27	116.9566

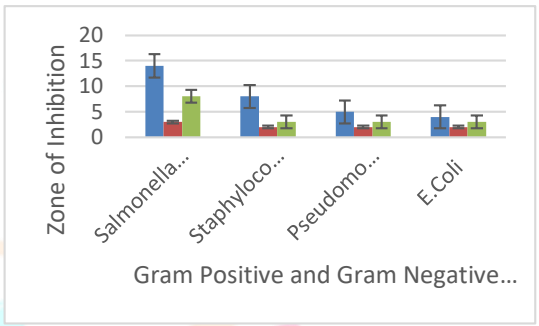

Fig.9: Comparative graphical representation of ZOIs of both Gram-positive and Gram-negative bacteria.

DPPH SCAVENGING ASSAY

Evaluation of antioxidant potentials of as-synthesized Silver Nanoparticle:

The antioxidant capacity of *P.reticulatus* stem bark-based silver nanoparticles was evaluated by DPPH (1, 1-diphenyl-2-picrylhydrazyle) free radical scavenging assay within 30 mins time. The purple-colored DPPH solution turned pale yellow with time when treated with AgNPs indicating the free radical scavenging activity of the nanoparticles tested. The Ag-NPs exhibited dose-dependent free radical scavenging potentials using the DPPH assay. The positive control ascorbic acid (25µg/mL) exhibited 76.53% scavenging capacity, while the negative control stem bark extract (1.0 %) exhibited 12.8% and these values were used for plotting the graph of antioxidant potentials of the as-synthesized silver nanoparticle.

Table3: Calculation of % RSA (Radical Scavenging Activity) and IC_{50} from DPPH Assay

Fig 10: Antioxidant capacity of positive control (ascorbic acid) at different concentrations (1–25 µg/mL) and negative control (stem bark extract). Values are mean ± SD.

The percent scavenging activity increased concurrently with the increase in the concentration of silver nanoparticles 1.0 to 24 µg mL^{-1}. The AgNP concentrations were tested within 30 min and the scavenging activity at the maximum concentration of 24 µg/mL was 60%. The percent scavenging capacities of the AgNPs were found to be 40.0, 44.04, 56.15, 65.38, 73.08, 85.58, and 93.27 % at 1, 2, 4, 8, 12, and 24 µg/mL respectively indicating their dose-dependent antioxidant potentials. The metallic $AgNO_3$ (1mM) showed a marginal value of 2.3% scavenging activity.

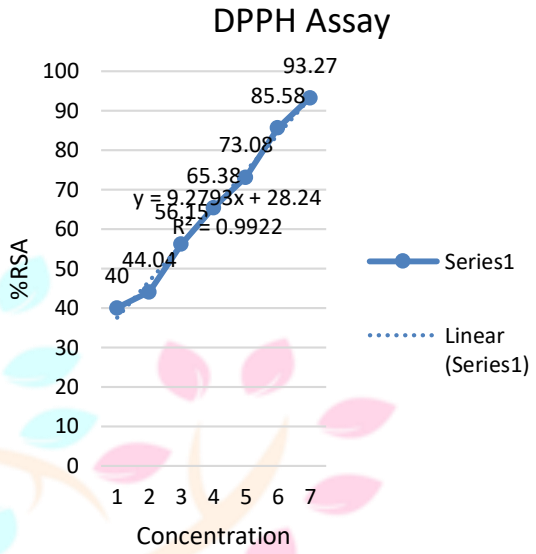

In-vitro cytotoxicity against Hela and MCF-7 cell lines

Only live cells reduce the tetrazolium dye but not the dead cells. When MTT is reduced, the quaternary amine is converted into a tertiary amine by opening the tetrazolium ring. A second tertiary amine, which is formed, binds to a hydrogen atom of the quaternary amine. The absorption spectrum of the molecule changes as a result of the displacement of this hydrogen atom at high pH. Subsequently, the cell numbers can be estimated. Thus, absorbance is directly correlated to the number of viable cells. The percentage cell toxicity of extract, Ag NPs against HeLa and MCF-7 cell lines. The data reveal that the increase in the concentration of extract increases toxicity. While comparing the results with other studies, it is obvious that higher toxicity is observed in aqueous extract, whereas in previous reports, other solvent extracts were found to have higher toxicity. One interesting observation is that the extract itself shows considerable toxicity against HeLa and MCF-7 cell lines. This may be due to the presence of phyllanthin, which is reported to be a potent anticancer drug.

MORPHOLOGICAL CHANGES OF HELA AND MCF-7 CELLS:

The morphological changes in HeLa and MCF-7 cells were examined using an inverted microscope. Treatments of HeLa and MCF-7 cells were performed with the IC50 of AgNPs (27.3 & and 34.3 µg/mL). The untreated control group exhibited a typical morphological shape, whereas AgNP-treated HeLa and MCF-7 cells did not. Furthermore, following exposure to AgNPs, many dead cells were observed. The number of live cells following treatment with the AgNPs was clearly decreased compared to that in the control sample, which agrees with previously reported results (Mittal et al., 2020).

In this study, Table 4 shows test compound is evaluated to analyze the cytotoxicity effect on HeLa and MCF-7 cell lines. The concentrations of the test compounds used to treat the cells are as follows:

Sl.No	Test Compounds	Cell lines	Concentration treated to cells
1	Untreated	HeLa & MCF-7	No treatment
2	Standard-Doxorubicin	HeLa & MCF-7	5uG/mL
3	Blank	-	Only Media without cells

4	Test	HeLa & MCF-7	5 (6.25, 12.5,25,50,100µg/mL)

Table 4: Details of test compound concentrations

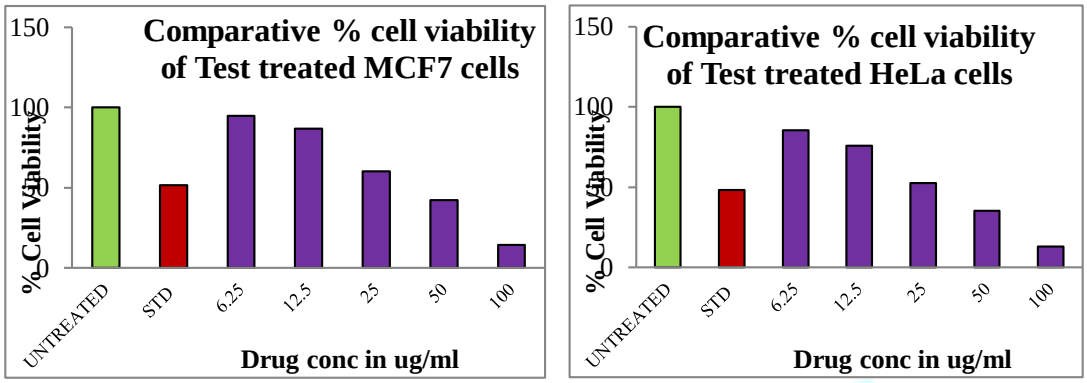

Figure 11: Percentage of cell viability test for HeLa and MCF-7 cell lines after 24 hours with AgNPs

Table 5: Cytotoxicity on Human breast and cervix cancer cells with IC_{50} values

Sl.No	Cell line	IC_{50} (uM/mL)±S.D
1	HeLa	**27.3**
2	MCF-7	**34.9**

Conclusion: The synthesis of AgNPs using P. reticulatus through a green chemistry approach with several advantages such as an economic, efficient, and ecofriendly process, which is also energy-efficient and cost-effective, results in healthier workplaces and communities, protecting human health and the environment, leading to less waste and safer products. The potentially active phytoconstituents involved in the Phyto-mediated synthesis of nanoparticles are biocompatible for a wide range of biomedical applications. Additionally, the nanoparticles were studied to show their antibacterial activity against Gram-positive and Gram-negative bacteria and antiproliferative effects on different human cancer cell lines, which were Hela, and MCF-7, in a dose-dependent manner. Thus, this report adds another feature to the medicinal hub plant P. reticulatus, i.e., its ability to successfully formulate AgNPs, which could be used effectively for their antibacterial, antioxidant, and antiproliferative properties.

Acknowledgments: The authors would like to acknowledge the financial support received from the Ministry of Tribal Affairs for Scheduled Tribes (RGNF-ST) for the award of a Junior Research Fellowship. The authors would also like to acknowledge the Department of Biochemistry, University College of Science, Hyderabad-07, India.

Disclosure statement: No potential conflict of interest was reported by the authors.

References:

- Ankanna, S.T.N.V.K.V.P., Prasad T.N.V.K.V., Elumalai E.K., Savithramma N., (2010). 'Production of biogenic silver nanoparticles using Boswellia ovalifoliolatastem bark'. Digest Journal of Nanomaterials and Biostructures, 5(2):369 – 372.
- Saxena, M., et al. (2017).' Pomegranate'. In: Horticultural Statistics at a glance. National Horticulture Board, Govt. of India,469.
- Abbaszadegan, A., Ghahramani, Y., Gholami, A., Hemmateenejad, B., Dorostkar, S., Nabavizadeh, M., & Sharghi, H. (2015). The Effect of Charge at the Surface of Silver Nanoparticles on Antimicrobial Activity against Gram-Positive and GramNegative Bacteria: A Preliminary Study. https://doi.org/10.1155/2015/720654
- Adamson, A. W., & Gast, A. P. (Alice P. (1997). Physical chemistry of surfaces. 784.

- Ahn, E. Y., Lee, Y. J., Park, J., Chun, P., & Park, Y. (2018). Antioxidant Potential of Artemisia capillaris, Portulaca oleracea, and Prunella vulgaris Extracts for Biofabrication of Gold Nanoparticles and Cytotoxicity Assessment. Nanoscale Research Letters, 13. https://doi.org/10.1186/s11671-018-2751-7
- Akintola, A. O., Kehinde, B. D., Ayoola, P. B., Adewoyin, A. G., Adedosu, O. T., Ajayi, J. F., & Ogunsona, S. B. (2020). Antioxidant properties of silver nanoparticles biosynthesized from methanolic leaf extract of Blighia sapida. IOP Conference Series: Materials Science and Engineering, 805(1). https://doi.org/10.1088/1757- 899X/805/1/012004
- Bonde SR, Rathod DP, Ingle AP, Ade RB, Gade AK, Rai MK (2012) Murraya koenigii—mediated synthesis of silver nanoparticles and its activity against three human pathogenic bacteria. Nanosci Methods 1:25–36
- Brunner TI, Wick P, Manser P, Spohn P, Grass RN, Limbach LK, Bruinink A, Stark WJ (2006) In vitro cytotoxicity of oxide nanoparticles: comparison to asbestos, silica, and effect of particle solubility. Env Sci Technol 40:4374–4381
- Chandran SP, Chaudhary M, Pasricha R, Ahmad A, Sastry M (2006) Synthesis of gold nanotriangles and silver nanotriangles using Aloe vera plant extract. Biotechnol Prog 22:577–579
- Chang W, Choi SCK, Soon SH, Bong KC, Hye JA, Min YL, Sang HP, Soo KK (2002) Antioxidant activity and free radical scavenging capacity between Korean medicinal plants and flavonoids by assay guided comparison. Plant Sci 163:1161–1168
- Dipankar C, Murugan S (2012) The green synthesis, characterization, and evaluation of the biological activities of silver nanoparticles synthesized from Iresine herbstii leaf aqueous extracts. Colloids Surf B 98:112–119
- Joshi M. Kaur S. Verma M. Mishra T. Analysis of antimicrobial activity of *Woodfordia fruticosa*, *Adhatoda vasica* and *Ricinus communis* against multi-drug resistant bacteria. Research Journal of Pharmacy and Technology. 2019;12(6):2987–94. DOI: 10.5958/0974-360X.2019.00505.5
- Saleh MM. Sadeq RA. Latif HKA. Abbas HA. Askoura M. Antimicrobial susceptibility and resistance profile of *Pseudomonas aeruginosa* isolates from patients at an Egyptian hospital. Research Journal of Pharmacy and Technology. 2018;11(8):3268–72. DOI: 10.5958/0974-360X.2018.00601.7
- Dixit A. Kumar N. Kumar S. Trigun V. Antimicrobial resistance: progress in the decade since emergence of New Delhi metallo-β- lactamase in India. Indian Journal of Community Medicine. 2019;44(1):4. DOI:10.4103/ijcm.IJCM_217_18
- Horbańczuk OK. Kurek MA. Atanasov AG. Brnčić M. Brnčić SR. The effect of natural antioxidants on the quality and shelf life of beef and beef products. Food Technology and Biotechnology. 2019;57(4):439. DOI: 10.17113/ftb.57.04.19.6267
- Sarker SD. Nahar L. An introduction to natural products isolation. Sarker S. Nahar L. Natural Products Isolation. vol 864. Humana Press.; 2012;1–25. https://doi.org/https://doi.org/10.1007/978-1- 61779-624-1_1
- Hussein RA. El-Anssary AA. Plants secondary metabolites: the key drivers of the pharmacological actions of medicinal plants. Herbal Medicine. 2019;1-13. DOI: 10.5772/intechopen.76139
- MTT Cell Proliferation Assay Instruction Guide – ATCC, VA, USA www.atcc.org
- Gerlier D., and N. Thomasset. J. Immunol. Methods 94: 57-63, 1986. Alley, M.C., et al.
- Cancer Res. 48: 589-601, 1988. Mosmann, T. J. Immunol. Methods 65: 55-63, 1983.
- Alley, M. C., Scudiere, D. A., Monks, A., Czerwinski, M., Shoemaker, R. II., and Boyd, M. R. Validation of an automated microculture tetrazolium assay (MTA) to assess growth and drug sensitivity of human tumor cell lines. Proc. Am. Assoc. Cancer Res., 27: 389, 1986
- *http://himedialabs.com/TD/CCK003.pdf*
- Mosmann T. Rapid colorimetric assay for cellular growth and survival: application to proliferation and cytotoxicity assays. J Immunol Methods. 1983; 65: 55–63.
- Bray, F.; Ferlay, J.; Soerjomataram, I.; Siegel, R.L.; Torre, L.A.; Jemal, A. Global cancer statistics 2018: GLOBOCAN estimates of incidence and mortality worldwide for 36 cancers in 185 countries. *CA A Cancer J. Clin.* **2018**, *68*, 394–424. [CrossRef] [PubMed]

- Vickers, A. Alternative cancer cures: "Unproven" or "disproven"? *CA A Cancer J. Clin.* **2004**, *54*, 110–118. [CrossRef] [PubMed]
- Wang, M.; Thanou, M. Targeting nanoparticles to cancer. *Pharmacol. Res.* **2010**, *62*, 90–99. [CrossRef] [PubMed]
- Chouhan, N. Silver nanoparticles: Synthesis, characterization and applications. In *Silver Nanoparticles-Fabrication, Characterization and Applications*; IntechOpen: London, UK, 2018; pp. 21–57.
- Nguyen, K.T. Targeted nanoparticles for cancer therapy: Promises challengesenge. *Nanomed. Nanotechnol.* **2011**. [CrossRef]
- Li, X.; Cui, R.; Liu, W.; Sun, L.; Yu, B.; Fan, Y.; Feng, Q.; Cui, F.; Watari, F. The use of nanoscaled fibers or tubes to improve the biocompatibility and bioactivity of biomedical materials. *J. Nanomater.* **2013**, *2013*. [CrossRef]
- Russell, A.; Hugo, W. 7 antimicrobial activity and action of silver. *Prog. Med. Chem.* **1994**, *31*, 351–370.
- Lee, S.H.; Jun, B.-H. Silver nanoparticles: Synthesis and application for nanomedicine. *Int. J. Mol. Sci.* **2019**,